ELSEVIER

Journal of Nuclear Materials 276 (2000) 235–242

journal of nuclear materials

www.elsevier.nl/locate/jnucmat

# Analysis of displacement cascades and threshold displacement energies in β-sic

J.M. Perlado[a], L. Malerba[a,*], A. Sánchez-Rubio[a], T. Díaz de la Rubia[b]

[a] *Instituto de Fusión Nuclear (DENIM), Universidad Politécnica de Madrid, C/ José Gutiérrez Abascal, 2, Madrid 28006, Spain*
[b] *Chemistry and Materials Division, Lawrence Livermore National Laboratory (LLNL), Livermore, CA 94550, USA*

**Abstract**

The threshold displacement energy (TDE) for both Si and C atoms in SiC at 300 K has been determined by means of molecular dynamics (MD) simulation along four crystallographic directions: [0 0 1], [1 1 0], [1 1 1] and $[\bar{1}\ \bar{1}\ \bar{1}]$. The existence of recombination barriers, which allow the formation of metastable defects even below the threshold, has been observed. Displacement cascades produced by both C and Si recoils of energies spanning from 0.5 keV up to, respectively, 5 and 8 keV have also been simulated with MD, both at 300 and 1300 K. Their analysis, together with the analysis of a damage accumulation at 1300 K, reveals that the two sublattices exhibit opposite responses to irradiation: whereas only a little damage is produced on the 'ductile' Si sublattice, many defects accumulate on the much more 'fragile' C sublattice. The low defect mobility in SiC prevents the study of defect evolution within the scope of MD. 

*PACS:* 61.82.-d; 61.82.Fk; 61.80.-*x*; 61.80.Hg

## 1. Introduction

Silicon carbide is a low activation material whose use, in different manufactured forms (porous tubes, SiC/SiC composites), has been proposed for the first wall and blanket of several concepts of Magnetic and Inertial Fusion reactors [1–7]. It is therefore of crucial importance to study extensively the effects of intensive neutron irradiation in this material.

So far, research programmes on SiC and SiC-based composites have dealt mostly with qualifying the material, mainly through experimental work [8]. Little has been done, however, with computer simulations, aimed at better understanding the basic principles of defect production and evolution at an atomistic level. It is this task that we started to deal with a few years ago and lately in a more systematic fashion.

In this paper, first we present the results obtained determining the threshold displacement energy (TDE) for Si and C atoms in SiC along different crystallographic directions and discuss the existence of recombination barriers. Then we report an analysis of the dynamics of displacement cascades produced by both Si and C recoils of energies up to, respectively, 8 and 5 keV. Finally, we mention some results of a preliminary study of damage accumulation in SiC.

## 2. Computational method

All simulations herein reported were carried out with the molecular dynamics (MD) simulation code MDCASK. This code, mainly developed at the LLNL in collaboration with other centres, among them the DENIM, offers the possibility of studying both metals [9], employing the embedded atom method potential [10,11], and covalent materials, namely Si, using the Stillinger–Weber potential [12,13], and SiC, using the Tersoff potential [14–17]. The latter has been demonstrated to be adequate to describe defect energetics in SiC [18]. It was used in our simulations in a recently optimised version [19], merged with a binary repulsive potential obtained from ab initio calculations [20], introduced to describe short-range (<0.5 Å) atomic interactions.

* Corresponding author. Tel.: +34-91 336 3108; fax:+34-91 336 3002.
*E-mail address:* malerba@denim.upm.es (L. Malerba)

0022-3115/00/$ - see front matter 
PII: S0022-3115(99)00183-X

MDCASK has been implemented in the Cray T3E massively parallel super-computer at the CIEMAT (Madrid, Spain): the implementation is based on the PVM message passing library and we have access to a maximum of 32 processors. On 16 processors the code runs at a rate of approximately 8 μs/atom/timestep.

All simulations were conducted at constant number of particles, volume and temperature (NVT ensemble). For the determination of the TDEs, a $6a_0 \times 6a_0 \times 7a_0$ box ($a_0 = 4.36$ Å), containing 2016 atoms, was used. For the simulation of displacement cascades and damage accumulation we used three boxes: $25a_0 \times 25a_0 \times 30a_0$ (150 000 atoms), $40a_0 \times 40a_0 \times 40a_0$ (512 000 atoms) and $40a_0 \times 40a_0 \times 60a_0$ (768 000 atoms), depending on the energy and type of recoil. The temperature was kept constant by employing the velocity rescaling method, applied to two or four boundary atom layers of the crystal box. Most results were obtained for 300 K, though a few cascades and the accumulation of damage were simulated at 1300 K. More details on the organisation of the simulations will be given in the relevant sections.

## 3. Threshold displacement energies and recombination barriers

It is well known that, above all in covalent solids, the TDE is markedly dependent upon direction. For this reason, we considered in our study four different directions already selected in earlier work [17,19], namely [0 0 1], [1 1 0], [1 1 1] and $[\bar{1}\ \bar{1}\ \bar{1}]$, and identified them by two different sets of angles: the geometrical ones and a pair of slightly modified angles (the corresponding modified directions were labelled as [***m]). For each direction we ran many cases, increasing the initial energy of the selected PKA by amounts of 1 eV (from less than 20 eV upward, depending on the direction). To get better statistics, we also repeated these cases setting the PKA into motion at different instants. In each simulation the equilibrium was reached in about 150 fs. At that point, a Si or C atom occupying the nearest position to the centre of the box was chosen as PKA and the evolution of the system was followed for about 5 ps.

In interpreting the results we assumed that the TDE was exceeded whenever a stable defect configuration was produced for all energies above the established threshold, regardless of this configuration involving the PKA itself or other atoms. Table 1 summarises our results.

As already reported in other papers [17,19,21], a remarkable difference is noticeable between the thresholds along the four different directions studied, a fact that reveals the conspicuous anisotropy of the TDE surface in SiC. It must be emphasized, though, that no big difference is generally found between geometrical and modified direction: this means that reasonably small departures from the exact crystallographic directions should not have such a misleading effect on experimental measurements of the TDEs.

The novelty of our results is the appearance of energy bands, *below* the established thresholds, within which a displacement is already produced. We attributed the occurrence of this phenomenon to the existence of *recombination barriers*, which allow the formation of metastable defect configurations (currently being studied with more accuracy), liable not to form if the PKA is given a higher energy. We also suppose that these *intermediate* defect configurations should not form at all at higher temperature: an investigation on this issue is currently being performed.

It is easy to verify that the TDEs reported in previous work [17,19] coincide mostly with the lower limits of the bands we mentioned. As a consequence, it turns out that the *real* Si-TDEs in SiC are generally higher than it was calculated before and are, on average, about twice as high as the C-TDEs along the same direction. Moreover, the PKA-energy bands over which the recombination barriers reveal their existence is wider on the Si sublattice than on the C sublattice (where, along certain directions, it is not even completely sure that such barriers exist). Hence, the formation of intermediate, metastable defects on the Si sublattice seems to be more likely than on the C sublattice. Overall, it appears to be much easier to create a stable displacement on the C sublattice than on the Si sublattice.

We would like to conclude this section observing that the existence of two thresholds leaves a question mark over which value should be used in DPA calculations. More generally, the question also arises of whether it makes sense at all to use the concept of DPA in non-metallic materials like silicon carbide.

## 4. Displacement cascades analysis

We simulated displacement cascades produced by both C and Si recoils whose energy spanned from 0.5 keV up to, respectively, 5 and 8 keV. The equilibrium at the desired temperature was reached after 1–2 ps. The Si or C atom chosen as PKA was then set into motion from the upper part of the box along a direction close to the [0 0 1] (the actual angles were changed randomly from simulation to simulation). After the PKA started moving, the evolution of the system was followed for a time varying between a few ps and ~1 ns. Most simulations were performed at 300 K, although some were conducted also at 1300 K.

It was observed that, even at 1300 K, the primary damage state (produced right after the recombination phase of the displacement cascade) is conserved practically unaltered for more than 1 ns. This seems to indicate that in SiC, owing to the very low mobility of

Table 1
Threshold displacement energies and PKA-energy ranges where the recombination barriers reveal their presence, for both Si and C recoils. In the last two columns a concise description of the defect configuration below (metastable) and above (stable) the threshold is given ($I_A$ = interstitial atom of type A, $V_A$ = vacancy site of type A, DB(AB) = dumbell formed by atoms A and B, $R_{AB}$ = replacement of a B-atom by an A-atom, $T_A$ = tetrahedral interstice among four A-atoms). The distance between the displaced atom and the closer vacancy is also specified, in lattice parameter units ($a_0 = 4.36$ Å)

| Recoil | Direction | Angles ($\theta$, $\varphi$) | TDE (eV) | Rec. barrier range (eV) | Metastable defect conf. | Stable defect conf. |
|---|---|---|---|---|---|---|
| Si | [0 0 1] | 0°; 0° | 56–59 | 35–36 → 43 | DB($I_{Si}$Si) + $V_{Si}$, $d_{I-V} \cong 0.80a_0$ | $R_{SiSi}$ + DB($I_{Si}$Si) + $V_{Si}$, $d_{R-V} \cong a_0$ |
| | [0 0 1m] | 2°; 44° | 60–61 | 35 → 39–45 | DB($I_{Si}$Si) + $V_{Si}$, $d_{I-V} \cong 0.80a_0$ | $R_{SiSi}$ + DB($I_{Si}$Si) + $V_{Si}$, $d_{R-V} \cong a_0$ |
| | [1 1 0] | 90°; 45° | 89–94 | 65–70 → 85–90 | DB($I_{Si}$Si) + $V_{Si}$, $d_{I-V} \cong 0.61a_0$ | $R_{SiSi}$ + DB($I_{Si}$Si) + $V_{Si}$, $d_{R-V} \cong 0.71a_0$ |
| | [1 1 0m] | 88°; 44° | 98–100 | 77 → 85 | DB($I_{Si}$Si) + $V_{Si}$, $d_{I-V} \cong 0.61a_0$ | $R_{SiSi}$ + DB($I_{Si}$Si) + $V_{Si}$, $d_{R-V} \cong 0.71a_0$ |
| | [1 1 1] | 55°; 45° | 42–44 | 31 → 36–38 | $I_C T_{Si}$ + $V_C$, $d_{I-V} \cong 0.76a_0$[a] | DB($I_C$Si) + $V_C$, $d_{I-V} \cong 1.13a_0^a$ |
| | [1 1 1m] | 45°; 44° | 43–45 | 32 → 41 | $I_C T_{Si}$ + $V_C$, $d_{I-V} \cong 0.76a_0^a$ | DB($I_C$Si) + $V_C$, $d_{I-V} \cong 1.13a_0^a$ |
| | [−1 −1 −1] | 125°; −135° | 110–112 | 38 → 75 | DB($I_{Si}$Si) + $V_{Si}$, $d_{I-V} \cong 0.75a_0$ | DB($I_{Si}$C) + $V_{Si}$, $d_{I-V} \cong 0.84a_0$ |
| | [−1 −1 −1m] | 135° ;−134° | 71–72 | 35–36 → 54–55 | DB($I_{Si}$Si) + $V_{Si}$, $d_{I-V} \cong 0.75a_0$ | DB($I_{Si}$C) + $V_{Si}$, $d_{I-V} \cong 0.84a_0$ |
| C | [0 0 1] | 0°; 0° | 30–32 | None | – | DB($I_C$C) + $V_C$, $d_{I-V} \cong 0.83a_0$ |
| | [0 0 1m] | 2°; 44° | 30–31 | None | – | DB($I_C$C) + $V_C$, $d_{I-V} \cong 0.83a_0$ |
| | [1 1 0] | 90°; 45° | 49–51 | 27 → 42 | DB($I_C$Si) + $V_C$, $d_{I-V} \cong 0.61a_0$ | DB($I_C$C) + $V_C$, $d_{I-V} \cong 0.91a_0$ |
| | [1 1 0m] | 88°; 44° | 54–56 | 27 → 45 | DB($I_C$Si) + $V_C$, $d_{I-V} \cong 0.61a_0$ | DB($I_C$C) + $V_C$, $d_{I-V} \cong 0.91a_0$ |
| | [1 1 1] | 55°; 45° | 29–31 | 20 → 25 | DB($I_C$Si) + $V_C$, $d_{I-V} \cong 0.62a_0$ | DB($I_C$C) + $V_C$, $d_{I-V} \cong 1.08a_0$ |
| | [1 1 1m] | 45°; 44° | 26–28 | 17 → 20 | DB($I_C$Si) + $V_C$, $d_{I-V} \cong 0.62a_0$ | DB($I_C$C) + $V_C$, $d_{I-V} \cong 1.08a_0$ |
| | [−1 −1 −1] | 125°; −135° | 57–61 | 45 → 52 | DB($I_C$Si) + $V_C$, $d_{I-V} \cong 0.64a_0$ | $R_{CSi}$+DB($I_{Si}$Si) + $V_C$, $d_{I-V} \cong 1.1a_0$ |
| | [−1 −1 −1m] | 135°; −134° | 57–58 | 47 → 49 | DB($I_C$Si) + $V_C$, $d_{I-V} \cong 0.64a_0$ | $R_{CSi}$ + DB($I_{Si}$Si)+$V_C$, $d_{I-V} \cong 1.1a_0$ |

[a] Along direction [1 1 1] the defect produced does not involve the Si recoil, rather the neighbouring C atom, which the PKA encounters at only 1.89 Å ($0.43a_0$) of distance.

defects, it would be possible to observe a change in the primary defect distribution only on timescales lying beyond the scope of MD. For this reason, it was decided to limit the extension of most simulations to a few ps.

Fig. 1 shows how the number of displacements produced by both Si recoils (Fig. 1(a)–(c)) and C recoils (Fig. 1(d)–(f)) depends upon the recoil energy at 300 K (since the effect of energy loss through electron excitation was not taken into account in the simulations, the recoil energy coincide with the damage energy). In Fig. 1(a) and (d) the number of displacements at the peak of the cascade is plotted, whereas Fig. 1(b) and (e) represent the number of displacements at saturation, that is at the end of the cascade. On average, about 20% of the atoms displaced at the peak regain their positions at saturation. It can be observed that the increase in the number of displacements versus energy appears to be described by a power exponent <1 (Fig. 1(a)). Such trend reminds the dependence typical of metals and is not surprising, since very high energy recoils should

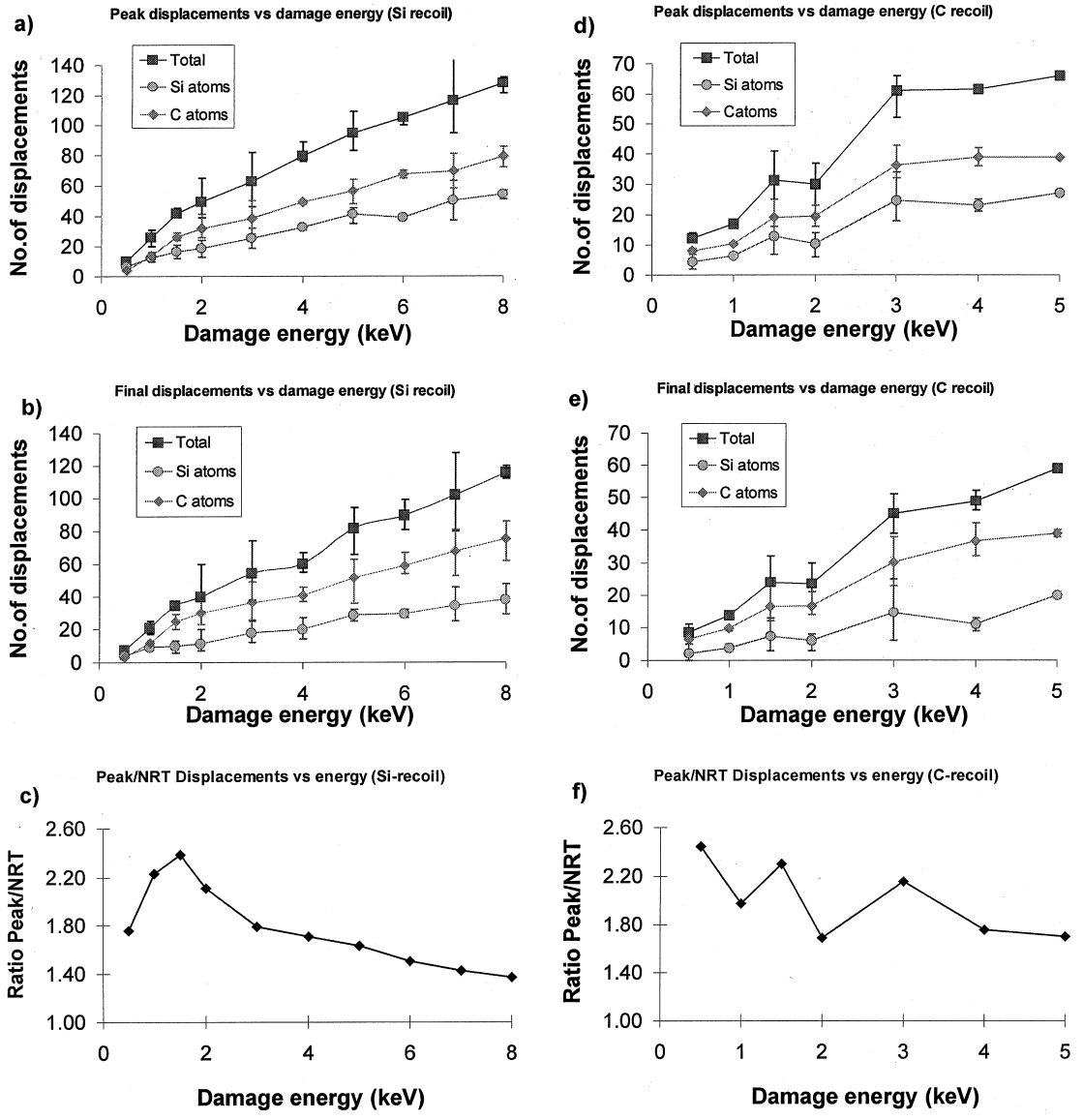


Fig. 1. Damage energy dependence of the displacement number in the case of Si recoils (a, b and c) and C recoils (d, e and f) at 300 K. (a) and (d) show the displacement number at the cascade peak, whereas (b) and (e) show it at saturation (i.e., at the end of the cascade). (c) and (f) compare the number of peak displacements calculated by MD simulations with the value calculated with the NRT method ($E_d \cong 35$ eV).

interact less with the atoms of the material, thereby having proportionally less chances of damaging its structure than lower energy recoils. Anyhow, simulations at higher energies are needed to draw definitive conclusions, because the apparent non-linear growth might also be due to a slope change at low energies of an otherwise linear law.

Turning to consider the differences between the effect of Si and C recoils, on average a C recoil produces 20–30% less displacements than a Si recoil of the same energy. Even more evident is the fact that a C recoil displaces less Si atoms than a Si recoil: at saturation, the average ratio Si-displaced-atoms/C-displaced-atoms is >0.5 for Si recoils and <0.4 for C recoils.

Finally, in Fig. 1(c) and (f) the numbers of peak displacements versus damage energy obtained by MD simulation at 300 K are compared with the values calculated with the NRT method [22]. In applying this method, we took a TDE of ≈35 eV. This value is the average of the lower limits of the recombination barriers ranges listed in Table 1. This choice was determined by the assumption that the interstitial atoms occupying metastable positions are to be included in the number of atoms displaced at the cascade peak. The surprising result of the comparison is that, contrary to what happens in the case of metals, the simulation yields more displacements than the NRT method and it looks like an agreement could be reached only at very high recoil energies. It is also interesting to note, in the case of Si recoils, the presence of a peak in the ratio Peak/NRT displacements around 1.5 KeV, probably a consequence of the non-linear law exhibited by the number of displacements versus energy around that value.

A similar study was conducted for the number of defects, namely vacancies and antisites (the number of interstitials is always very close to that of vacancies, therefore the conclusions drawn here are alike in the two cases). The results are shown in Fig. 2 for both Si recoils (Fig. 2(a) and (b)) and C recoils (Fig. 2(c) and (d)). In the case of the number of vacancies (Fig. 2(a) and (c)), the increase versus energy seems to exhibit a downward curvature even more pronounced than in the case of the number of displacements. The average proportion of C and Si vacancies changes depending on the type of recoil: in the case of Si recoils about 30% of the total are Si vacancies, this value dropping to only 20% for C recoils. Moreover, 25% less vacancies are produced, on average, by C recoils and there is a slight

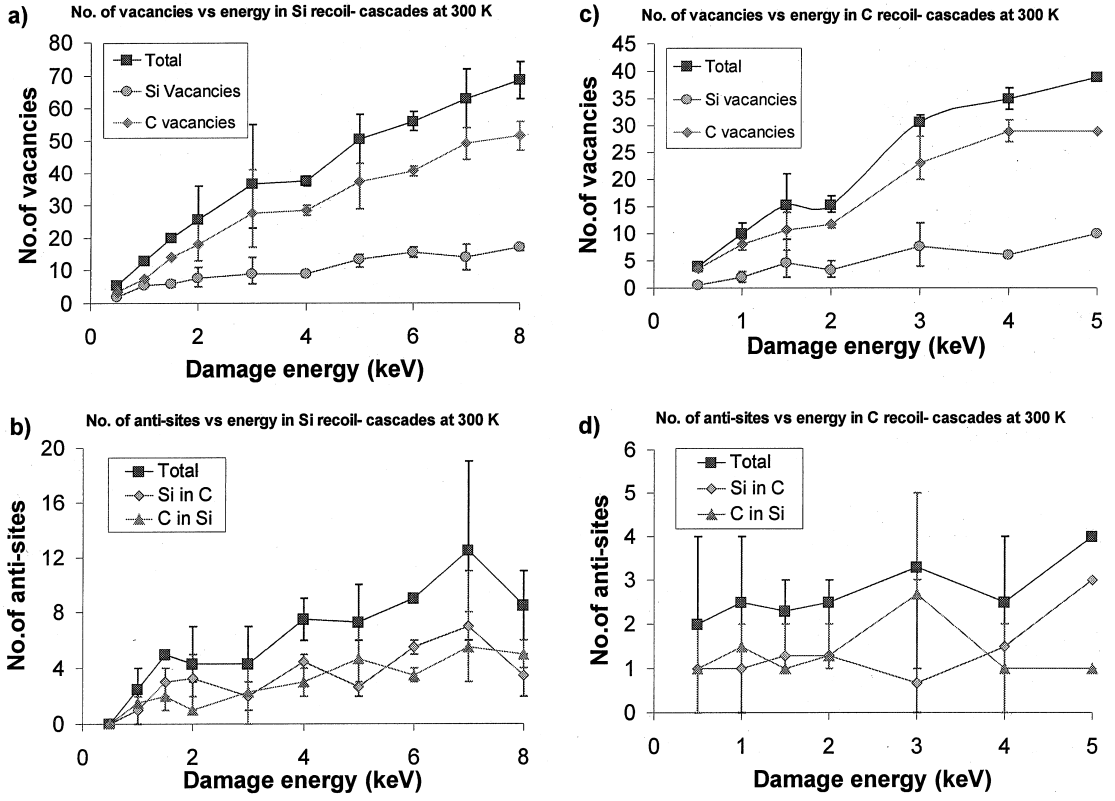


Fig. 2. Dependence upon damage energy of the number of defects in the case of Si recoils (a and b) and C recoils (c and d) at 300 K. (a) and (c) show the number vacancies versus energy, whereas (b) and (d) show the number of antisites versus energy.

tendency of the ratio Si-vacancies/C-vacancies to decrease with growing energy.

The same curves for the antisites (Fig. 2(b) and (d)) appear to be much less significant, probably because their number remains too low for a clear law to be interpolated over the range of energies considered here. It looks like the number of antisites grows very slowly with increasing recoil energy and that C recoils produce about 50% less defects of this type than Si recoils of the same energy. Furthermore, according to these results it seems that the production of Si and C antisites is, on average, equally probable.

We conclude this section with Fig. 3, where an idea is given of what the primary damage state looks like from the point of view of vacancy clustering. We considered that two defects form a cluster when their distance is equal to or smaller than the distance between third neighbours. This choice was dictated by the following considerations: (a) if clusters of vacancies of the same type have to be included, it is necessary to select a threshold clustering distance greater than the second neighbour distance (3.08 Å); (b) the difference between third and second neighbour distance is so small (0.54 Å) that it appeared unjustified to locate there the threshold; (c) third neighbours are the last ones contained in a sphere of radius smaller than $a_0 = 4.36$ Å. It can be seen that big clusters have a very low occurrence, even at fairly large energies, and definitely most vacancies appear to be isolated. Anyway, the formation of multivacancies cannot be completely ruled out. We know that these clusters of vacancies survive for time spans longer than 1 ns. What we do not know yet is whether they are actually stable, that is whether, over timescales exceeding the scope of MD, they would dissolve into isolated vacancies or not.

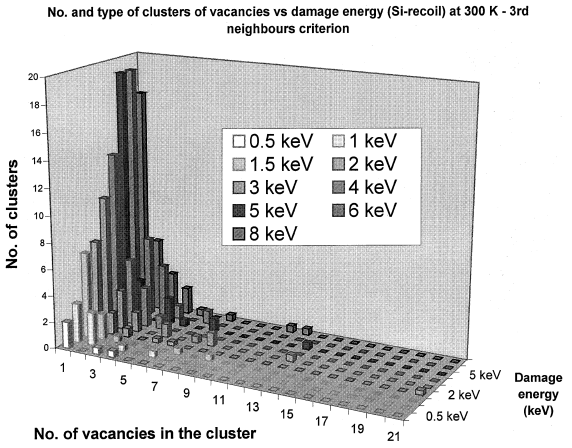


Fig. 3. Number of vacancy clusters versus size (number of vacancies contained) and damage energy, at 300 K. Clusters were defined using a 3rd neighbour criterion.

## 5. Damage accumulation

The main interest of simulating a situation of damage accumulation lies in studying whether any tendency to saturation in the number of defects is visible in a condition of linear production of displacements. With this aim in mind, we repeated and extended a study reported in [23]. We give here a short summary of what we observed. More details can be found in [21].

After 3 ps of equilibration at 1300 K, 25 Si recoils of 500 eV (first simulation) and 1 keV (second simulation) were introduced at a rate of 1 recoil every 3 ps. This corresponds to a huge damage rate, about $2 \times 10^7$ DPA/s, although over the whole simulation only about $1.75 \times 10^{-3}$ DPA were accumulated. After 3 ps from the appearance of each PKA, before introducing the next one, a picture of the situation inside the crystal was

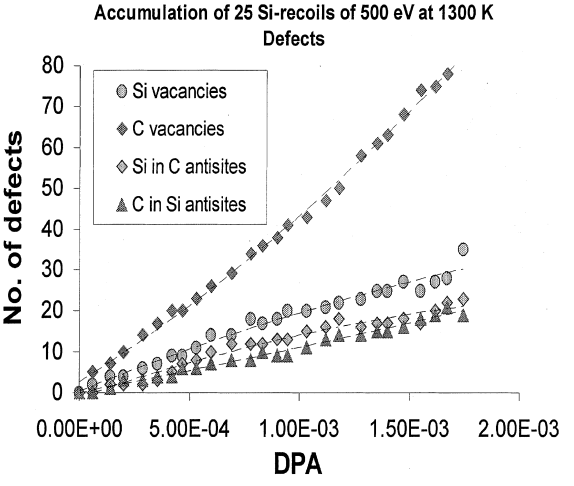


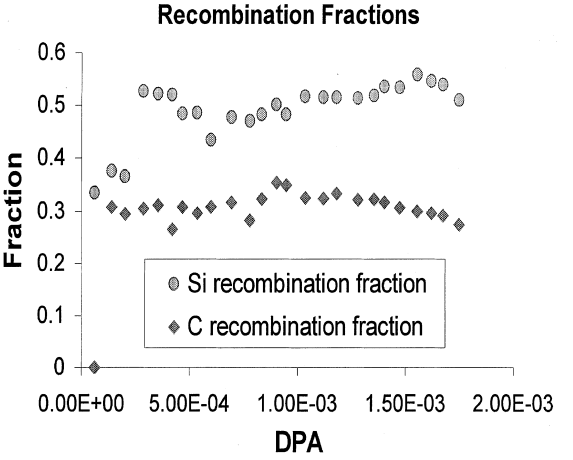


Fig. 4. Defect number and recombination fractions as a function of DPA in Si and C sublattices in a damage accumulation at 1300 K.

taken by performing a quenching. After the 25th PKA, an annealing of the system was carried out at 1300 K for 100 ps but, as expected, no substantial alteration of the damage state produced at the end of the accumulation was observed.

In Fig. 4, which refers to the first simulation, our most interesting results are summarised. What is most striking is the overwhelming majority of C vacancies with respect to any other type of defect (Si vacancies, antisites), in a proportion of about 4:1. Furthermore, trying to fit the data to a curve, it resulted that, while both Si vacancies and antisites grow according to a linear law, C vacancies exhibit a non-negligible quadratic increase, responsible for about 1/3 of the growth at the end of the simulation. The explanation of this behaviour lies patently in the different capability of recombination displayed by the two sublattices. As it is, by plotting the recombination fractions (number-of-recombinations/number-of-displaced-atoms) versus DPA, it appears clear that not only is the Si sublattice recombination capability much higher (>0.5 versus ~0.3), but also that the recombination fraction in the C sublattice dwindles faintly, thereby explaining the quadratic increase in the number of C vacancies.

## 6. Conclusions

The TDEs for Si and C atoms in SiC at 300 K have been determined with the accuracy permitted by MD. Si-TDEs in SiC turn out to be generally higher than it had been calculated before and are, on average, about twice as high as C-TDEs along the same direction. The existence of recombination barriers allows the formation of metastable defect configurations even below the threshold.

Displacement cascades produced by both C and Si recoils up to, respectively, 5 and 8 keV have been simulated at 300 and 1300 K. A situation of damage accumulation has also been simulated. In all cases, many more defects were produced on the C sublattice than on the Si sublattice.

The Si sublattice shows a tendency to absorb most of the damage energy in the form of lattice excitation, instead of defect production, and exhibits an outstanding capability of recombination. This causes little disorder to be produced on this particularly 'ductile' sublattice. The high value of the Si-TDEs herein reported and the existence of recombination barriers do not contrast with the above-stated feature of the Si sublattice, but in fact endorse it. As it is, the production of stable defects on the Si sublattice is made more difficult and probably most defects are metastable, so that their recombine more easily.

On the contrary, the C sublattice appears to be much more 'fragile': C vacancies are fairly easily produced and their number increases more than linearly in damage accumulation conditions. Moreover, the proportion of C defects to Si defects increases when the recoil is a C atom, as well as with increasing recoil energy.

Finally, it has been seen that the primary damage state produced in the material after the recombination phase of the displacement cascades, characterised by the presence of relatively few clusters of defects, is conserved practically unaltered for timescales lying beyond the scope of MD. This fact is probably due to the low mobility of defects in SiC. Thus, to study their evolution it becomes essential to turn to diffusion simulations.

## Acknowledgements

The authors are grateful to M.J. Caturla and E. Alonso (LLNL) for their indispensable aid all along the months devoted to the carrying out of this work; to C. Alejaldre (CIEMAT) for having made it possible to carry it out; to the European Commission, for the financial support (Marie Curie Research Training Grant, Fusion Programme, Contract No. ERB 5004-CT97-5002). Work also performed under the auspices of the US Department of Energy by LLNL under contract W-7405-Eng-48.

## References

[1] S. Sharafat, F. Najmabadi, Fus. Eng. Des. 18 (1991) 215.
[2] A.S. Pérez Ramírez, A. Caso, L. Giancarli, N. Le Bars, G. Chaumat, J.F. Salavy, J. Szczepansky, J. Nucl. Mater. 233–237 (1996) 1257.
[3] Y. Kosaky, Conceptual design and economic evaluation of laser power plant KOYO, Proc. of ICENES (1993) p. 76.
[4] B. Badger et al., HIBALL, A conceptual heavy ion beam driver fusion reactor study, Kernforschungszentrum Karlsruhe Report KfK-3202 – Madison, Univ. of Wisconsin Fusion Technology Institute, Report UWFDM-450, June 1981; HIBALL II, An improved conceptual heavy ion beam driver fusion reactor study, KfK-3840 – FPA-84-4 – UWFDM-625, July 1985.
[5] B. Badger et al., Preliminary conceptual design of SIRIUS, A symmetric illumination direct drive laser fusion reactor – Progress Report, Univ. of Wisconsin Fusion Technology Institute, Report UWFDM-568, 1984.
[6] B. Badger et al., LIBRA, A light ion beam fusion conceptual reactor design, Univ. of Wisconsin Fusion Technology Institute, Report UWFDM-800, 1984.
[7] McDonnel Douglas Aerospace Team, Inertial fusion energy reactor design studies – Final Report, vol. I, II and III, DOE/ER-54101 MDC92E0008, March 1992.
[8] See e.g., Proc. from First and Second IEA International Workshop on SiC/SiC Ceramic Composites for Fusion Applications, (1st) 28–29 October, 1996 Ispra (VA), Italy, (2nd) 23–24 October, 1997 Sendai, Japan.

[9] T. Díaz de la Rubia, M.W. Guinan, J. Nucl. Mater. 174 (1990) 151.
[10] S.M. Foiles, M.I. Baskes, M.S. Daw, Phys. Rev. B. 33 (12) (1986) 7893.
[11] M.W. Finnis, J.E. Sinclair, Philos. Mag. A 50 (1984) 45.
[12] F.H. Stillinger, T.A. Weber, Phys. Rev. B 31 (1985) 5262.
[13] M.J. Caturla, T. Díaz de la Rubia, G.H. Gilmer, Mater. Res. Soc. Symp. Proc. 316 (1994) 141.
[14] J. Tersoff, Phys. Rev. B 39 (1989) 5566.
[15] J. Tersoff, Phys. Rev. Lett. 64 (1990) 1757.
[16] J. Tersoff, Phys. Rev. B 49 (1994) 15150.
[17] J. Wong, T. Díaz de la Rubia, M.W. Guinan, M. Tobin, J.M. Perlado, J. Sanz, J. Nucl. Mater. 251 (1997) 98.
[18] H. Huang, N.M. Ghoniem, J.K. Wong, M.I. Baskes, Modell. Simul. Mater. 251 (1997) 98.
[19] R. Devanathan, T. Díaz de la Rubia, W.J. Weber, J. Nucl. Mater. 253 (1998) 47.
[20] K. Nordlund, N. Runeberg, D. Sundholm, Nucl. Instrum. Meth. 132 (1997) 45.
[21] J.M. Perlado, L. Malerba, T. Díaz de la Rubia, MD Fus. Techn. 34 (1998) 840.
[22] M.J. Norgett, M.T. Robinson, I.M. Torrens, Nucl. Eng. Des. 33 (1975) 50.
[23] T. Díaz de la Rubia, J.M. Perlado, M. Tobin, J. Nucl. Mater. 233–237 (1996) 1523.